Oxidation of Coordinated Ammonia to Nitrosyl in the Reaction of Aqueous Chlorine with *cis*-$[Ru(bpy)_2(NH_3)_2]^{2+}$

Zerihun Assefa[†] and David M. Stanbury*

Contribution from the Department of Chemistry, Auburn University, Auburn, Alabama 36849

Received September 25, 1996[⊗]

Abstract: Rapid-scan stopped-flow kinetic studies show that the multielectron oxidation of coordinated ammonia in *cis*-$[Ru(bpy)_2(NH_3)_2]^{2+}$ by acidic (pH 0.5−1.3) aqueous chlorine provides the nitrosyl complex *cis*-$[Ru(bpy)_2(NH_3)(NO)]^{3+}$ as the final product. The first step in this process involves the metal-centered oxidation of *cis*-$[Ru(bpy)_2(NH_3)_2]^{2+}$ to *cis*-$[Ru(bpy)_2(NH_3)_2]^{3+}$, and the rate law for this process is $-d[Ru(II)]/dt = 2k_1[Ru(II)][Cl_2]$ with the second order rate constant, k_1, as $(1.1 \pm 0.1) \times 10^3$ M^{-1} s^{-1}. Independent studies conducted on the *cis*-$[Ru(bpy)_2(NH_3)_2]^{3+}$ complex show that conversion to the nitrosyl complex follows an A → B → C type consecutive pathway with k_{slow} and k_{fast} components, respectively. In the pH range of 0.5−2.8, the k_{slow} process follows a competitive pathway where both Cl_2 and HOCl react with deprotonated coordinated ammonia. The rate law for the k_{slow} process has the form $k_{slow} = \{(k_2[H^+][Cl^-] + k_3K_{Cl})/(K_{Cl} + [H^+][Cl^-])\}([Cl_2]_{tot}/[H^+])$, where K_{Cl} corresponds to the equilibrium constant for the hydrolysis of Cl_2. The rate constant k_2, corresponding to the Cl_2 term, is 6.5 ± 0.3 s^{-1} while the rate constant k_3, corresponding to the HOCl reaction, is 2.0 ± 0.2 s^{-1}. The k_{fast} process involves further oxidation of intermediate B by Cl_2. The intermediate of this reaction is speculated as either a nitrene, nitrido, or chloroamine complex. The kinetic studies indicate that the conversion of this unidentified intermediate to the final nitrosyl complex proceeds through a fast preequilibrium, involving deprotonation of the intermediate, followed by a direct attack by Cl_2. The rate law corresponding to the k_{fast} process has the form $k_{fast} = [k_4K_{int}[Cl_2]_{tot}[H^+][Cl^-]]/[\{K_{int} + [H^+]\}\{[H^+][Cl^-] + K_{Cl}\}]$, the equilibrium constant K_{int} for the deprotonation process is 0.11 ± 0.04 M, and the rate constant k_4 is $(7.8 \pm 1.5) \times 10^2$ M^{-1} s^{-1}.

Introduction

Oxidation of ammonia by nitrifying bacteria such as *Nitrosomonas europaea* is an important component of the global nitrogen cycle.[1] These bacteria use the copper-dependent enzyme ammonia monooxygenase to catalyze the conversion to hydroxylamine:[2]

$$NH_3 + O_2 + 2e^- \rightarrow NH_2OH + H_2O \qquad (1)$$

One might hope to gain some insight into this process by examining the oxidation of metal-coordinated ammonia in aqueous synthetic systems, but the data are quite limited.

Most commonly, oxidation of coordinated ammonia leads to nitrosyl complexes, and this has been achieved chemically with $[Ru(NH_3)_6]^{3+}$ by use of dilute $HClO_4$ at steam-bath temperatures[3] and alkaline Cl_2/NH_3 mixtures, O_2, and H_2O_2 at room temperature.[4,5] No suggestions were made regarding the mechanism in the $HClO_4$ report,[3] while the evolution of NO_2 vapors during the reaction led to the suggestion of a complex mechanism in the Cl_2/NH_3 report.[4] More concrete information was presented in the report of oxidation by O_2 and H_2O_2, where it was established that oxidation took place through attack at coordinated ammonia.[5] In other chemical studies it has been shown that oxidation of $[Os(NH_3)_6]^{3+}$ by Ce(IV) leads to an intermediate nitrido complex, and here too it can safely be assumed that the ammonia is coordinated when oxidized.[6] Nitrido complexes are formed in the hypochlorite oxidation of Cr(III) porphyrins in the presence of ammonia, but it is unclear whether the ammonia is coordinated during the oxidative step.[7] Similar remarks apply to the formation of a nitrido complex of phthalocyaninatomanganese(V).[8] Formation of a dinitrogen complex occurs in the reaction of NO with $[Ru(NH_3)_6]^{3+}$.[9,10] Isotopic tracer and kinetic studies imply that the mechanism involves attack of NO at $[Ru^{III}(NH_3)_5(NH_2)]^{2+}$ with subsequent dehydration. Dinitrogen complexes are also formed in the reaction of NO with $[Os^{IV}(NH_3)_nX_{6-n}]^{(n-2)+}$ complexes, and qualitative evidence indicates a mechanism similar to the analogous reaction of $[Ru(NH_3)_6]^{3+}$.[11] Albeit in nonaqueous media, chemical oxidation of a bis(ammine) cofacial ruthenium(II) diporphyrin leads to N−N bond formation, ultimately yielding a bridged dinitrogen complex.[12] Qualitative observations indicate that this reaction goes by way of one-electron oxidation of both metal centers, followed by amine deprotonation and N−N linkage. In early studies it was shown that dichloramido complexes ($Pt^{IV}-NCl_2$) are formed in the reaction of hypochlorite with $[Pt^{IV}(NH_3)_3Cl_3]^+$ and related compounds.[13,14] The rate laws for these reactions were interpreted

* Author to whom correspondence should be addressed.
[†] Present Address: Oak Ridge National Laboratory, Chemical and Analytical Science Division, P.O. Box 2008, Oak Ridge, TN 37831-6375.
[⊗] Abstract published in *Advance ACS Abstracts,* January 1, 1997.

(1) Kuenen, J. G.; Robertson, L. A. In *The Nitrogen and Sulphur Cycles*; Cole, J. A., Ferguson, S. J., Eds.; Cambridge University Press: New York, 1988; pp 161−218.
(2) Ensign, S. A.; Hyman, M. R.; Arp, D. J. *J. Bacteriol.* **1993**, *175*, 1971−1980.
(3) Broomhead, J. A.; Taube, H. *J. Am. Chem. Soc.* **1969**, *91*, 1261.
(4) Schreiner, A. F.; Lin, S. W.; Hauser, P. J.; Hopcus, E. A.; Hamm, D. J.; Gunter, J. D. *Inorg. Chem.* **1972**, *11*, 880−888.
(5) Pell, S. D.; Armor, J. N. *J. Am. Chem. Soc.* **1975**, *97*, 5012−5013.
(6) Buhr, J. D.; Winkler, J. R.; Taube, H. *Inorg. Chem.* **1980**, *19*, 2416−2425.
(7) Buchler, J. W.; Dreher, C.; Lay, K.-L.; Raap, A.; Gersonde, K. *Inorg. Chem.* **1983**, *22*, 879−884.
(8) Grunewald, H.; Homborg, H. *Z. Naturforsch. B* **1990**, *45*, 483−489.
(9) Pell, S.; Armor, J. N. *J. Am. Chem. Soc.* **1972**, *94*, 686−687.
(10) Pell, S. D.; Armor, J. N. *J. Am. Chem. Soc.* **1973**, *95*, 7625−7633.
(11) Buhr, J. D.; Taube, H. *Inorg. Chem.* **1980**, *19*, 2425−2434.
(12) Collman, J. P.; Hutchison, J. E.; Ennis, M. S.; Lopez, M. A.; Guilard, R. *J. Am. Chem. Soc.* **1992**, *114*, 8074−8080.
(13) Kukushkin, Y. N. *Russ. J. Inorg. Chem.* **1965**, *10*, 846−848.
(14) Kukushkin, Y. N. *Russ. J. Inorg. Chem.* **1965**, *10*, 848−852.

S0002-7863(96)03362-8 CCC: $14.00

in terms of rate-limiting attack of OCl^- at $Pt^{IV}-NH_3$, which presents conceptual difficulties because of the lack of an available site for attack. Thus, there appear to be no kinetic studies of the oxidation of coordinated ammonia to an oxonitrogen species.

Electrochemically, coordinated NH_3 has been oxidized to nitrosyls at $[Ru(trpy)(bpy)(NH_3)]^{2+}$,[15] $[Os^{II}(trpy)(bpy)NH_3]^{2+}$,[16] $[Os^{II}(trpy)(Cl)_2(NH_3)]$,[17,18] and $[Ru(NH_3)_2(bpy)_2]^{2+}$.[19] In the case of $[Ru(trpy)(bpy)(NH_3)]^{2+}$ it was shown that the first step is one-electron oxidation to $[Ru(trpy)(bpy)(NH_3)]^{3+}$, which is followed by its disproportionation to give an imido complex.[15] The corresponding Os(II) complex behaves differently, in that after oxidation to Os(III) rate-limiting deprotonation followed by one-electron oxidation leads to an Os(IV) imido intermediate.[16] Chemical trapping experiments have verified the occurence of this Os(IV) imido intermediate.[20] A third mechanistic variation is seen in the oxidation of $[Os^{II}(trpy)(Cl)_2(NH_3)]$:[17] a sequence of two reversible one-electron oxidations to Os(IV), followed by a proton-coupled two-electron oxidation to $[Os^{VI}(trpy)(Cl)_2N]^+$. Further oxidation to the nitrosyl was achieved in acetonitrile through reaction with $ON(CH_3)_3$.[18] Yet another mechanism is indicated for the oxidation of $[Ru(NH_3)_2(bpy)_2]^{2+}$, where one-electron oxidation to Ru(III) is followed by an electrode-specific 5-electron oxidation to the nitrosyl product.[19] Formation of N_2 has been demonstrated in the electrochemical oxidation of $[(bpy)_2(NH_3)RuORu(NH_3)(bpy)_2]^{4+}$.[21] Here, one-electron oxidation is followed by a proton-coupled 5-electron process. Despite the great progress in these electrochemical studies, no kinetic data have been reported.

Herein we present the first study of the kinetics and mechanism of a chemical oxidation of coordinated ammonia to a nitrosyl complex: we find evidence that oxidation by aqueous Cl_2 and HOCl is activated rather than protected by coordination of ammonia to a metal center.

Experimental Section

Reagents. Water was doubly deionized and distilled from a Barnstead Fi-stream glass still. Lithium perchlorate ($LiClO_4 \cdot 3H_2O$) was prepared by neutralizing Li_2CO_3 (Fisher) with concentrated $HClO_4$. The solution was heated to boiling in order to remove any dissolved CO_2 gas. Slow cooling provided the crystalline product. The product was washed several times with cold water in order to remove the excess acid (until a neutral pH was attained). The salt was further recrystallized twice from water and dried in air. LiCl (Fisher) was also recrystallized twice from water. Both the $LiClO_4$ and LiCl solutions were standardized by passing a known amount through a Dowex 50W-X8 cation-exchanger and titrating against a KHP standardized NaOH solution. Stock solutions of NaOCl were prepared by bubbling Matheson high-purity Cl_2 gas, prewashed in 0.1 M $KMnO_4$ and then in concentrated H_2SO_4,[22] into a 0.6 M NaOH solution. This solution was then diluted with an additional volume of NaOH to raise the pH to 12. This solution was assayed at 292 nm ($\epsilon = 350\ M^{-1}\ cm^{-1}$)[23] and stored at ca. −5 °C in a polyethylene Nalgene bottle which had been aged by previous exposure to a hypochlorite solution. The bpy (2,2′-bipyridine) ligand was purchased from Aldrich and was recrystallized twice by adding hexane (2:1 (v/v)) to a saturated solution in CH_2Cl_2 and cooling the mixture in a freezer.

Synthesis of *cis*-$[Ru(bpy)_2(NH_3)_2](ClO_4)_2$. This compound was synthesized by slightly modifying the literature procedure.[24] First, *cis*-$Ru(bpy)_2Cl_2$ was synthesized by the following adaptation of a literature method.[25] $RuCl_3 \cdot 3H_2O$ (807.4 mg, 3.1 mmol), 962.5 mg (6.2 mmol) of bpy, and 0.9 g of LiCl were dissolved in 7 mL of *N*,*N*-dimethylformamide. The solution was refluxed for 8 h and cooled to room temperature. After adding 35 mL of acetone, the solution was kept in a freezer over night. The dark-greenish crystalline product was filtered while cold and washed with H_2O (2.5 mL × 3) and then with ether (2.5 mL × 3) and dried in air. Yield: 61%. When the synthesis was conducted in a 2:5 MeOH−dimethylformamide mixture the yield increased to 73%.

A 0.332-g (0.7 mmol) sample of *cis*-$Ru(bpy)_2Cl_2$ was suspended in $MeOH/H_2O$ (3:1 (v/v)) and 4 mL of aqueous NH_3 solution (sp gr = 0.9 g/mL) was added. The suspension was then refluxed for 2 h in a water bath which was maintained at ca. 70 °C. The dark red solution was filtered while hot, heated in a water bath until all the MeOH evaporated, and concentrated to one fourth of its original volume. The solution was then allowed to cool to room temperature and loaded onto a column of (ca. 20 cm in length and 1 cm in diameter) SP-C25 Sephadex (40−120 μm bead size) in the acid form. The sample was eluted with 0.2 M HCl. The initial yellow band was rejected while the middle dark brown band was collected at a rate of 2 mL/min. A green band remained at the top of the column. The eluted solution was then concentrated to ca. 5 mL in a rotary evaporator. Addition of ice-cold saturated $NaClO_4$ provided an immediate dark red precipitate. The precipitate was filtered, washed with ice-cold water (ca. 2 mL) and then with Et_2O, and dried in a desiccator. (*Warning! In one experiment a small quantity of the material exploded and caught fire during removal from a sintered glass funnel.*) The product was further purified by recrystallization where Et_2O was added dropwise to a MeOH solution until a permanent cloudiness was observed. Dark brown shining crystals were obtained after keeping the solution overnight in a freezer. Yield based on Ru is 76%. ^1H NMR (DMSO-d_6, δ vs TMS): 9.1 (2H, d), 8.7 (2H, d), 8.5 (2H, d), 8.1 (2H, t), 7.8 (4H, t), 7.4 (1H, d), 7.2 (2H, t), 2.9 (3H (NH_3), s). Anal. Calcd for $C_{20}N_6H_{26}O_{10}Cl_2Ru$: C, 35.20; H, 3.84; N, 12.31. Found: C, 36.42; H, 4.08; N, 12.00.

Synthesis of *cis*-$[Ru(bpy)_2(NH_3)(NO)](ClO_4)_2Cl \cdot 3H_2O$. A 0.1-g sample of *cis*-$[Ru(bpy)_2(NH_3)_2][ClO_4]_2$ was dissolved in 0.1 M HCl (ca. 20 mL) and Cl_2 gas was bubbled through the solution. The initial violet color changed to light yellow immediately. The excess Cl_2 gas was then removed by bubbling Ar gas through the solution. Complete removal of the solvent via rotary evaporator provided light yellow flakes. Single crystals were grown by slow evaporation (∼4 weeks) of the HCl solution at room temperature. IR ν(NO) in Nujol mull: 1944 cm^{-1}. ^1H NMR (DMSO-d_6, δ vs TMS): 9.3 (1H, d), 9.2 (1H, d), 9.1 (1H, d), 9.0 (3H, m), 8.8 (1H, t), 8.7 (1H, t), 8.5 (2H, m), 8.2 (1H, t), 8.1 (1H, t), 7.7 (3H, m), 7.3 (1H, d), 5.8 (3H (NH_3), s). Anal. Calcd for $C_{20}N_6H_{25}O_{12}Cl_3Ru$: C, 32.08; H, 3.36; N, 11.22. Found: C, 32.49; H, 3.33; N, 11.10. An alternative route to this complex, as the PF_6^- salt, was reported by Callahan and Meyer,[26] while Lai and Wong reported the synthesis of the $CF_3SO_3^-$ salt.[19]

Synthesis of *cis*-$[Ru(bpy)_2(NH_3)_2](ClO_4)_3$. A 155-mg sample of *cis*-$[Ru(bpy)_2(NH_3)_2](ClO_4)_2$ was dissolved in 10 mL of 0.5 M HCl. To this solution was added 30 mg of MnO_2 and the suspension was stirred vigorously. After about 10 min the dark red mixture turned to light violet. The mixture was then stirred for an additional 1 h, the excess MnO_2 was filtered off, the solvent was evaporated on a rotary evaporator, and the residue was stored in a freezer. At room temperature the compound as a solid has been found unstable. The Ru(III) solutions for the kinetic studies were prepared *in situ* by using

(15) Thompson, M. S.; Meyer, T. J. *J. Am. Chem. Soc.* **1981**, *103*, 5577−5579.
(16) Murphy, W. R.; Takeuchi, K.; Barley, M. H.; Meyer, T. J. *Inorg. Chem.* **1986**, *25*, 1041−1053.
(17) Pipes, D. W.; Bakir, M.; Vitols, S. E.; Hodgson, D. J.; Meyer, T. J. *J. Am. Chem. Soc.* **1990**, *112*, 5507−5514.
(18) Williams, D. S.; Meyer, T. J.; White, P. S. *J. Am. Chem. Soc.* **1995**, *117*, 823−824.
(19) Lai, Y.-K.; Wong, K.-Y. *J. Electroanal. Chem.* **1994**, *374*, 255−261.
(20) Coia, G. M.; White, P. S.; Meyer, T. J.; Wink, D. A.; Keefer, L. K.; Davis, W. M. *J. Am. Chem. Soc.* **1994**, *116*, 3649−3650.
(21) Ishitani, O.; White, P. S.; Meyer, T. J. *Inorg. Chem.* **1996**, *35*, 2167−2168.
(22) Cooper, J. N.; Margerum, D. W. *Inorg. Chem.* **1993**, *32*, 5905−5910.
(23) Johnson, D. W.; Margerum, D. W. *Inorg. Chem.* **1991**, *30*, 4845−4850.
(24) Bryant, G. M.; Fergusson, J. E.; Powell, H. K. J. *Aust. J. Chem.* **1971**, *24*, 257−273.
(25) Sullivan, B. P.; Salmon, D. J.; Meyer, T. J. *Inorg. Chem.* **1978**, *17*, 3334−3341.
(26) Callahan, R. W.; Meyer, T. J. *Inorg. Chem.* **1977**, *16*, 574−581.

$HClO_4$ instead of HCl. After weighing and dissolving the Ru(II) species in $HClO_4$, excess MnO_2 was added, and the suspension was stirred for ca. 15 min and filtered into a volumetric flask containing appropriate amounts of solutions of the various compounds used in the kinetic study. The Ru(III) solutions were freshly prepared for each run of the kinetic study and used within 0.5−1 h. No deterioration of the sample was observed during this time, as the Ru(III) solution is easily and quantitatively reduced back to the Ru(II) system by ascorbic acid providing the characteristic *cis*-$[Ru(bpy)_2(NH_3)_2]^{2+}$ peak at 490 nm.

Intrumental Methods. UV−vis spectra were recorded on an HP 8452A diode array spectrophotometer with a 1-cm quartz cell. pH measurements were conducted at room temperature on a Corning pH meter, Model 130, with a Corning semi-micro combination glass electrode filled with 3 M NaCl. Standard electrochemical measurements were carried out in nitrogen-purged solutions with 0.1 M $HClO_4$ or $LiClO_4$ as supporting electrolyte. Cyclic voltammetry (CV) and Osteryoung square wave voltammetry (OSWV) were performed with a BAS-100 electrochemical analyzer employing a conventional three-electrode cell with a platinum disk working electrode, a platinum wire auxiliary electrode, and an Ag/AgCl reference electrode. Some electrochemical studies were also conducted using a glassy carbon working electrode. Solutions contained ∼1 mM of the ruthenium complexes. E_f values for the complexes correspond to the $E_{1/2}$ values in CV and E_p values in OSWV measurements. They are reported relative to NHE using a value of 0.197 V as $E°$ for the Ag/AgCl couple.

The initial studies were single wavelength kinetics conducted on a Hi-Tech Scientific stopped flow apparatus, Model SF-51, equipped with an SU-40 spectrophotometer unit. The temperature was maintained at 25 °C with a C-400 circulating water bath. The absorbance decrease at 490 nm was monitored by mixing equal volumes of the *cis*-$[Ru(bpy)_2(NH_3)_2]^{2+}$ and Cl_2 solutions to give a reaction mixture with concentration of ca. 0.1 mM of the ruthenium(II) system. The output from the SU-40 unit was collected by an On-line Instruments (OLIS) 4300 data acquisition system based on a Zenith computer. The rate constants were evaluated by exponential fits with the OLIS subroutines. The final studies were conducted on the OLIS rapid scanning monochromator (RSM 1000) with a dual-beam UV−vis recording and a global fitting subroutine.

In order to minimize loss of the Cl_2 gas by volatility, the NaOCl solution was drawn into an air tight glass syringe, equipped with a small magnetic bar and containing appropriate amounts of the $HClO_4$, Cl^-, and $LiClO_4$ solutions. The solution was stirred for a few minutes and part of it was injected into a quartz cell. For experiments at high acidity the Cl_2 content was immediately measured spectroscopically at 325 nm ($\epsilon = 70\ M^{-1}\ cm^{-1}$),[27] and the HOCl concentration was determined from the absorbance at 254 nm ($\epsilon = 59\ M^{-1}\ cm^{-1}$).[28] For experiments at pH >1 and without added Cl^-, the HOCl concentration was determined from the absorbance at 254 nm and $[Cl_2]_{tot}$ was taken as the initial hypochlorite concentration. The remaining solution was used for the kinetics study. For each run the actual Cl_2 concentration was measured at the beginning of the experiment and used in the calculation of $[Cl_2]_0$. Measurements conducted at the end of the kinetics experiment indicated that loss of Cl_2 by this technique is less than 2%. Reactions were initiated by mixing equal volumes of the two reactants, both of which were maintained at 0.5 M ionic strength using $LiClO_4$ as the background electrolyte. In all of the kinetics studies solutions were permitted to contact platinum, glass, and Teflon only. For the Ru(II) system the spectral profile changes were followed in both the visible and UV regions and the kinetics was analyzed using the global fitting subroutine of the RSM 1000 system. For the Ru(III) reaction the spectral changes were monitored in the UV region (320−440 nm) by use of the RSM 1000 system, and were further analyzed using the Specfit software package.[29]

Measurement of p*K* for the Equilibrium *cis*-$[Ru(bpy)_2(NH_3)NO]^{3+} + H_2O \rightleftharpoons$ *cis*-$[Ru(bpy)_2(NH_3)NO_2]^+ + 2H^+$. The p*K* value for the nitrosyl−nitro equilibrium was determined spectroscopically at 25 °C in water at $I = 0.5$ M ($LiClO_4$). Constant pH was maintained in the experiment by using KH_2PO_4 as a buffer. An aliquot of an aqueous solution of *cis*-$[Ru(bpy)_2(NH_3)NO]^{3+}$ was added to each of twelve 50-mL flasks (containing appropriate amounts of $LiClO_4$ and KH_2PO_4 solutions of 0.5 and 0.01 M, respectively) to give a complex concentration of ca. 2×10^{-4} M. An aliquot of 0.1 M $HClO_4$ or NaOH was added to this solution in order to vary the pH in the range of 3−6. The solutions were allowed to sit for 5 h, since preliminary experiments indicated a significant change of the absorbance with time suggesting that the equilibration is a slow process. After 5 h the absorbance of the solution remained constant. After recording the pH, each solution was then measured spectrophotometrically where the absorbance at 432 nm was especially noted. The nitrosyl complex is essentially transparent at 432 nm and only the nitro species absorbs significantly, which leads to a yellow coloration at higher pH.

Table 1. Spectroscopic Properties of the Ruthenium Compounds

compd	$E_{1/2}$, V[a]	λ_{max}, nm ($10^{-3}\epsilon$, $M^{-1}\ cm^{-1}$)[b]
cis-$[Ru(bpy)_2(NH_3)_2]^{2+}$	0.86	486 (8.9) 346 (7.3) 292 (> 50) 244 (19.1)
cis-$[Ru(bpy)_2(NH_3)_2]^{3+}$		334 sh (3.9) 320 (20.9) 246 (21.3)
cis-$[Ru(bpy)_2(NH_3)NO]^{3+}$	0.34	328 (10.0) 296 (19.5) 242 sh (22.0)
cis-$[Ru(bpy)_2(NH_3)NO_2]^+$		432 (6.9) 328 (6.9) 288 (49.0) 242 (15.6)

[a] V vs NHE in 0.1 M $LiClO_4$ at 25 °C with 1 mM $[Ru]_{tot}$. [b] Absorption measurements were conducted in 0.1 M $HClO_4$.

Results

UV−vis Spectra. The absorption data of the compounds are shown in Table 1. The *cis*-$[Ru(bpy)_2(NH_3)_2]^{2+}$ has the characteristic[24] Ru(II) → π^* (bpy) absorption bands at 486 and 346 nm in aqueous solution. These bands are slightly red-shifted in MeOH and appear at 496 and 352 nm, respectively. The bpy $\pi \rightarrow \pi^*$ transition is observed at 292 nm and shows no significant solvatochromic shift. Upon oxidation of *cis*-$[Ru(bpy)_2(NH_3)_2]^{2+}$ by Ce(IV), PbO_2, or MnO_2 the band at 486 nm disappears and a weak shoulder appears at 334 nm. As shown in Figure 1, the absorbance of the bpy $\pi \rightarrow \pi^*$ band decreases significantly, and is observed at a red-shifted position of 302 nm (with a shoulder at 312 nm) upon metal-centered oxidation. As evaluated from the absorption spectral change, chemical oxidation of the *cis*-$[Ru(bpy)_2(NH_3)_2]^{2+}$ by Ce(IV), PbO_2, and MnO_2 provides a metal-centered oxidation where re-reduction with SO_3^{2-}, NO_2^-, and Zn/amalgam provides the starting material. On the other hand, oxidation of *cis*-$[Ru(bpy)_2(NH_3)_2]^{2+}$ by Cl_2 and Br_2 leads to a product, identified as the nitrosyl complex, *cis*-$[Ru(bpy)_2(NH_3)NO]^{3+}$, which is not reduced back to the starting diamine species by the above reductants. Spectroscopically, the major characteristic difference between *cis*-$[Ru(bpy)_2(NH_3)_2]^{3+}$ and *cis*-$[Ru(bpy)_2(NH_3)NO]^{3+}$ lies in the absorption band changes observed in the mid-UV region. The absorbance of the weak shoulder at 334 nm, in the *cis*-$[Ru(bpy)_2(NH_3)_2]^{3+}$ system, increases and a well-resolved distinct band appears at 328 nm for the nitrosyl complex. In addition the band at 312 nm is absent in the nitrosyl complex and the band at 302 nm blue shifts to 296 nm (Figure 1) when compared to the diammine species. These changes have allowed

(27) Wang, T. X.; Kelly, M. D.; Copper, J. N.; Beckwith, R. C.; Margerum, D. W. *Inorg. Chem.* **1994**, *33*, 5872−5878.
(28) Zimmerman, G.; Strong, F. C. *J. Am. Chem. Soc.* **1957**, *79*, 2063−2066.
(29) Binstead, R. A.; Zuberbühler, A. D., SPECFIT, 1995, Spectrum Software Associates, Chapel Hill, NC.

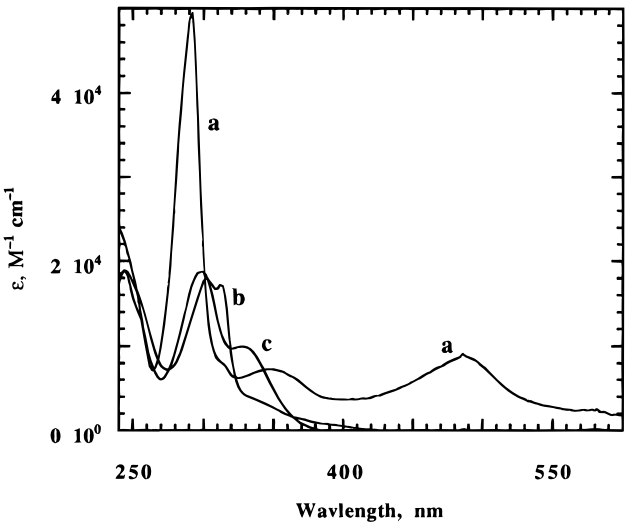

Figure 1. Comparison of the spectral profiles of (a) *cis*-$[Ru(bpy)_2(NH_3)_2]^{2+}$, (b) *cis*-$[Ru(bpy)_2(NH_3)_2]^{3+}$, and (c) *cis*-$[Ru(bpy)_2(NH_3)NO]^{3+}$. The spectra were recorded in 0.1 M $HClO_4$.

us to follow the kinetics of oxidation of coordinated ammonia to a nitrosyl ligand.

NMR Data. The ^{1}H NMR spectral data of *cis*-$[Ru(bpy)_2(NH_3)_2]^{2+}$ are given in the Experimental Section, and the peaks are assigned according to the following diagram:

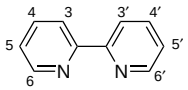

When compared to the free uncoordinated ligand, the H6 proton of the *cis*-$[Ru(bpy)_2(NH_3)_2]^{2+}$ complex shows a significant downfield shift (8.7 and 9.1 ppm, respectively), which is consistent with a cis arrangement where the π-cloud of the adjacent ligand induces a diamagnetic anisotropic effect. The ^{1}H NMR data clearly indicate that the pyridines within each bpy ligand in *cis*-$[Ru(bpy)_2(NH_3)_2]^{2+}$ are magnetically nonequivalent.[30−32] As a result, out of the possible 8-proton resonance peaks, seven distinct bands were observed in DMSO solvent with the peaks for the H5 and H4′ protons overlaping.

The ^{1}H NMR spectral data of the nitrosyl complex, *cis*-$[Ru(bpy)_2(NH_3)NO]^{3+}$, are given in the Experimental Section. Replacing one of the *cis*-NH_3 ligands by a nitrosyl reduces the symmetry of the molecule and, thus, the two bpy ligands are placed in nonequivalent environments. The effect of this reduced symmetry is clearly evident from the ^{1}H NMR spectra. Out of a total of 16 nonequivalent protons of the two bipyridyl rings, 12 distinct resonance peaks were observed in the NMR spectrum, with the other proton resonances giving an overlaping signal. Moreover, a dramatic downfield shift in the NH_3 protons was observed in the *cis*-$[Ru(bpy)_2(NH_3)NO]^{3+}$ species when compared to *cis*-$[Ru(bpy)_2(NH_3)_2]^{2+}$ (5.8 and 2.9 ppm, respectively), and indicates a significant electron cloud depletion at the metal center as a result of a strong back-bonding interaction with the nitrosyl ligand. In addition, the absence of any paramagnetic induced shift or broadening in the NMR data shows that the metal center is in a 2+ oxidation state (diamagnetic) and that the additional positive charge resides on the nitrosyl ligand, NO^+. This is consistent with the Enemark−Feltham generalization[33] that $\{Ru-NO\}^6$ complexes are diamagnetic and that the nitrosyl group is formally bound as NO^+ to Ru(II).

Cyclic Voltammetry Studies. The cyclic voltammogram of *cis*-$[Ru(bpy)_2(NH_3)_2]^{2+}$ in 0.1 M $HClO_4$ shows a reversible one-electron wave with $E_{1/2}$ at 0.86 V vs NHE. This value is comparable to that reported in 0.1 M CF_3CO_2H at a glassy carbon electrode.[19] No further oxidation of the *cis*-$[Ru(bpy)_2(NH_3)_2]^{3+}$ occurs upon scanning the potential to 1.2 V. Scanning the potential at various rates, ranging from 10 to 200 mV/s, has no effect on the shape of the voltammogram other than slightly increasing the $\Delta E_{p/p}$ potential (from 64 to 75 mV). The cyclic voltammogram of the nitrosyl complex, *cis*-$[Ru(bpy)_2(NH_3)NO]^{3+}$, in 0.1 M $HClO_4$ shows a reversible reduction wave with $E_{1/2}$ at 0.34 V vs NHE ($\Delta E_{p/p}$ = 64 mV) for the ligand-centered $\{Ru^{II}-NO^+/Ru^{II}-NO\}$ couple. No further oxidation of the *cis*-$[Ru(bpy)_2(NH_3)NO]^{3+}$ system occurs upon scanning the potential to 1.2 V. Varying the scan speed from 10 to 100 mV/s also does not cause any unusual alteration of the voltammogram. In addition to the CV studies, Osteryoung square-wave voltammetric measurements (OSWV) were conducted in order to assess the purity of our samples. These measurements gave no evidence for the presence of more than one species in the solution, and potentials similar to the CV studies were obtained for all the complexes reported in this paper.

Nitrosyl/Nitro Conversion. The acid−base equilibrium in the nitrosyl−nitro interconversion of *cis*-bis(bipyridyl)ruthenium(II) complexes has been studied previously,[19,34,35] and has been shown to occur as in

$$cis\text{-}[Ru(bpy)_2(L)NO]^{3+} + H_2O \rightleftharpoons cis\text{-}[Ru(bpy)_2(L)NO_2]^{+} + 2H^{+} \quad (2)$$

Spectral changes accompanying this reaction for L = NH_3 are shown in Figure 2, and show that the product, *cis*-$[Ru(bpy)_2(NH_3)NO_2]^+$, is characterized by an absorbance maximum at 432 nm. The spectrophotometric titration curve at this wavelength (Figure 2, inset) shows that above pH 4.5 the nitro form exists in significant amounts at equilibrium. As shown in Figure 3, a plot of 1/absorbance vs $[H^+]^2$ is linear indicating that the reaction is an overall two-proton process rather than the stepwise single-proton process as shown in eqs 2a and 2b:

$$cis\text{-}[Ru(bpy)_2(L)NO]^{3+} + H_2O \rightleftharpoons cis\text{-}[Ru(bpy)_2(L)NO_2H]^{2+} + H^{+} \quad (2a)$$

$$cis\text{-}[Ru(bpy)_2(L)NO_2H]^{2+} \rightleftharpoons cis\text{-}[Ru(bpy)_2(L)NO_2]^{+} + H^{+} \quad (2b)$$

Note that in the corresponding *trans* complexes where L = OH^- and Cl^- steps 2a and 2b are resolved.[36] From the slope and intercept of the plot in Figure 3 we derive a p*K* value of 11.3 for the net two-proton reaction. In the two examples of *cis*-$[Ru(bpy)_2(L)NO]^{3+}$ species reported previously[34,35] the p*K* values for L = Cl^- and pyridine correspond to 18.8 and 8.0, respectively, and bracket our intermediate p*K* value of 11.3 for L = NH_3. The wide variation in the acidity of these systems

(30) Lytle, F. E.; Petrosky, L. M.; Carlson, L. R. *Anal. Chim. Acta* **1971**, *57*, 239−247.
(31) Spotswood, T. M.; Tanzer, C. I. *Aust. J. Chem.* **1967**, *20*, 1227−1242.
(32) Bryant, G. M.; Fergusson, J. E. *Aust. J. Chem.* **1971**, *24*, 441−444.
(33) Enemark, J.; Feltham, R. D. *Coord. Chem. Rev.* **1974**, *13*, 339−406.
(34) Godwin, J. B.; Meyer, T. J. *Inorg. Chem.* **1971**, *10*, 2150−2153.
(35) Keene, F. R.; Salmon, D. J.; Walsh, J. L.; Abruña, H. D.; Meyer, T. J. *Inorg. Chem.* **1980**, *19*, 1896−1903.
(36) Togano, T.; Kuroda, H.; Nagao, N.; Maekawa, Y.; Nishimura, H.; Howell, F. S.; Mukaida, M. *Inorg. Chim. Acta* **1992**, *196*, 57−63.

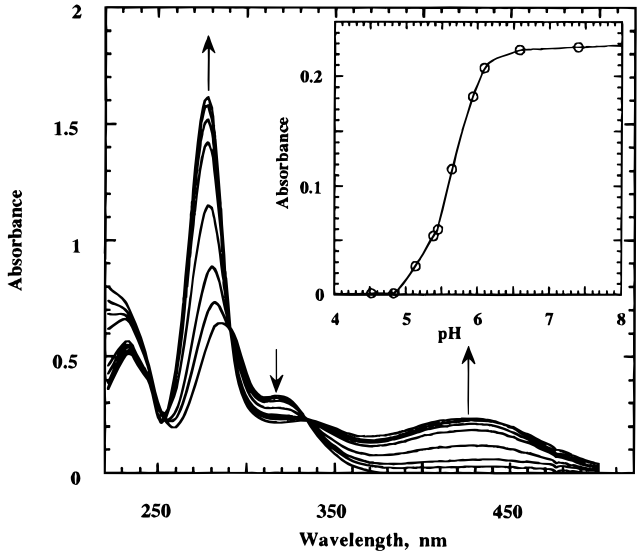

Figure 2. Spectral profile change with pH in the conversion of *cis*-$[Ru(bpy)_2(NH_3)NO]^{3+}$ to *cis*-$[Ru(bpy)_2(NH_3)NO_2]^+$. The concentration of *cis*-$[Ru(bpy)_2(NH_3)NO]_0^{3+}$ is 2×10^{-4} M; KH_2PO_4 (buffer) = 0.01 M; μ = 0.5 M ($LiClO_4$). The inset is a plot of the absorbance at 432 nm vs pH, with the solid line drawn as an arbitrary curve to guide the eye.

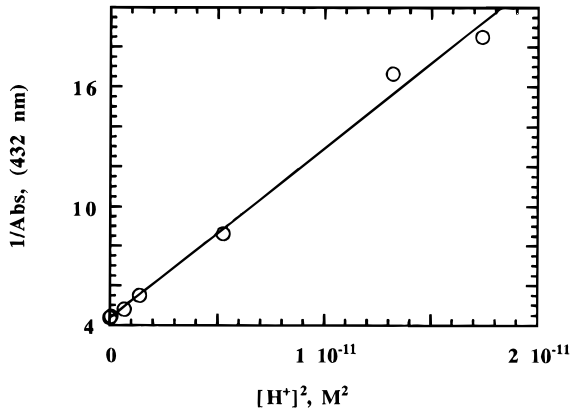

Figure 3. Plot of 1/absorbance vs $[H^+]^2$ for the nitrosyl−nitro interconversion. The absorbance value corresponds to the 432 nm measurement. The linear dependence observed in the figure clearly indicates that the calculated p*K* value (reaction 2) corresponds to a two-proton process. Experimental conditions are as given in Figure 2.

with a change in the cis-coordinated ligand, L, parallels the change in the $E_{1/2}$ value for the corresponding $[RuNO]^{3+}/[RuNO]^{2+}$ couple and clearly is a consequence of the electron-deficient nature of the NO group. The $E_{1/2}$ values for L = py, NH_3, and Cl^- are 0.49,[35] 0.34 (this work), and 0.15,[26] respectively (the literature values reported against SCE were recalculated against NHE) and as described above parallel the acidity of the complexes.

Kinetics: **Reaction of *cis*-$[Ru(bpy)_2(NH_3)_2]^{2+}$ with Cl_2.** Rapid-scan stopped-flow studies of the reaction between *cis*-$[Ru(bpy)_2(NH_3)_2]^{2+}$ and aqueous chlorine show that the first step corresponds to the one-electron oxidation to the *cis*-$[Ru(bpy)_2(NH_3)_2]^{3+}$ intermediate, presumably as in

$$2\ cis\text{-}[Ru(bpy)_2(NH_3)_2]^{2+} + Cl_2 \rightarrow 2\ cis\text{-}[Ru(bpy)_2(NH_3)_2]^{3+} + 2Cl^- \quad (3)$$

In acidic media the reaction is fast, reaching completion in less than 0.5 s. A series of rapid-scan spectra recorded in the 420−550-nm range at a rate of 1000 scans/s over a 0.25 s time period for the reaction with excess chlorine shows a smooth monotonic loss of the absorbance arising from Ru(II) and no evidence for an isosbestic point, the conditions being $[Ru(II)]_0 = 0.05$ mM, $[Cl^-] = 0.1$ M, $[H^+] = 0.10$ M, $[Cl_2]_{tot} = 7.6$ mM, $\mu = 0.5$ M ($LiClO_4$), and $T = 25$ °C. In Table 2 is shown the dependence of the rate of this reaction on $[Cl_2]_{tot}$ and $[H^+]$. The data show a first-order dependence on $[Cl_2]_{tot}$. Moreover, in the pH range of 0.5−1.3, the pseudo-first-order rate constants are unaffected by $[H^+]$ and added $[Cl^-]$. Thus the rate law for this reaction is given by

Table 2. Kinetic Dependence of the One-Electron Oxidation of *cis*-$[Ru(bpy)_2(NH_3)_2]^{2+}$ on $[H^+]$ and $[Cl_2]^a$

$[H^+]$, M	$[Cl_2]_{tot}$, mM	k_{obs}, s^{-1}	$10^{-3}(2k_1)$, $M^{-1}\ s^{-1}$
0.05	7.0	14.7	2.1
0.08	7.5	15.7	2.1
0.10	7.6	15.0	2.0
0.12	7.0	15.0	2.1
0.14	7.7	15.7	2.1
0.16	7.1	15.5	2.2
0.20	8.0	17.3	2.2
0.30	7.5	16.2	2.2
0.10	7.2	15.0	2.1
0.10	5.2	10.8	2.1
0.10	2.8	6.6	2.3
0.10	7.8	16.0	2.1
0.10	7.3	14.9[b]	2.0
0.10	6.4	13.0[c]	2.0

[a] Conditions: $[cis\text{-}[Ru(bpy)_2(NH_3)_2]^{2+}]_0 = 0.05-0.08$ mM, $\mu = 0.5$ M ($LiClO_4$), and 25 °C. $[Cl^-]$ was maintained at 0.2 M. [b] $[Cl^-] = 0.15$. [c] $[Cl^-] = 0.05$ M.

$$-d[Ru(II)]/dt = 2k_1[Ru(II)][Cl_2]_{tot} \quad (4)$$

and, under large excess of $[Cl_2]_{tot}$

$$k_{obs} = 2k_1[Cl_2]_{tot} \quad (5)$$

where $[Cl_2]_{tot} = [Cl_2] + [HOCl]$ because of the hydrolysis of chlorine as in

$$Cl_2 + H_2O \rightleftharpoons HOCl + H^+ + Cl^- \qquad K_{Cl} \quad (6)$$

Since the p*K* for the hydrolysis of Cl_2 (eq 6) is ca. 3,[37] the concentration of HOCl is negligible in the pH range that the kinetics studies have been conducted, and thus eq 5 can be rewritten in terms of aqueous molecular Cl_2 as

$$k_{obs} = 2k_1[Cl_2] \quad (5')$$

From the data shown in Table 2, the second-order rate constant, k_1, corresponds to $(1.1 \pm 0.1) \times 10^3\ M^{-1}\ s^{-1}$.

A rigorous treatment of the equilibria in aqueous chlorine solutions should also consider the presence of Cl_3^-, which exists through the following rapid equilibrium:

$$Cl^- + Cl_2 \rightleftharpoons Cl_3^- \qquad K_{Cl3} \quad (7)$$

Wang et al. have reported a value of 0.18 M^{-1} for K_{Cl3}, which implies that Cl_3^- never contributes significantly to mass balance in any of the experiments reported herein.[27] The fact that rate law 5′ is independent of $[Cl^-]$ shows that Cl_3^- does not compete significantly with Cl_2 in the reaction with *cis*-$[Ru(bpy)_2(NH_3)_2]^{2+}$.

When the reaction is monitored in the UV region (300−420 nm) a more complicated behavior is observed, where, in addition

(37) Wang, T. X.; Margerum, D. W. *Inorg. Chem.* **1994**, *33*, 1050−1055.

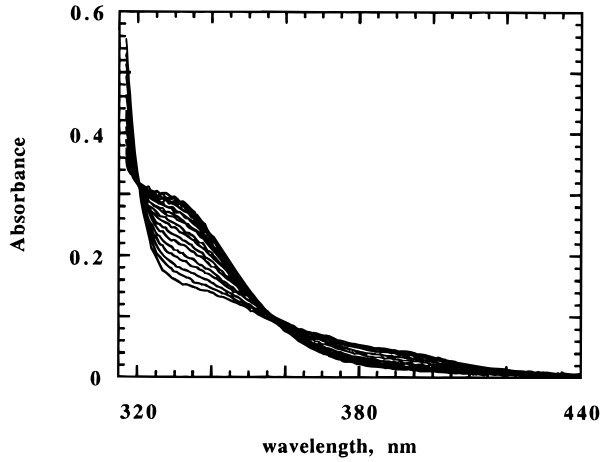

Figure 4. OLIS rapid-scan spectra showing the change in the absorbance in the UV region for the reaction of *cis*-$[Ru(bpy)_2(NH_3)_2]^{3+}$ with Cl_2. Original data were collected in 120-ms intervals, for a total of 15 s, and are shown in 0.72-s intervals. Conditions: $[Ru(III)]_0 =$ 0.05 mM; $[Cl^-] = 0.2$ M; $[H^+] = 0.29$ M; $[Cl_2]_{tot} = 8.9$ mM; $\mu = 0.5$ M ($LiClO_4$); 25 °C.

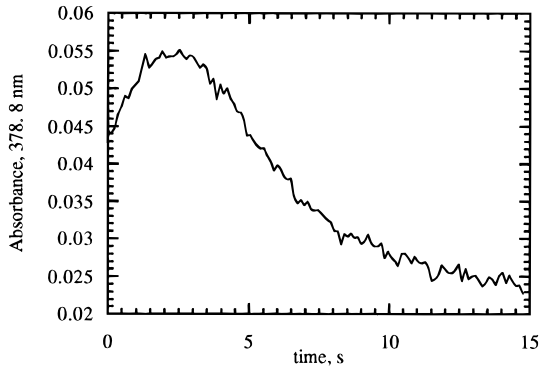

Figure 5. Kinetic time trace at 378.8 nm for the reaction between *cis*-$[Ru(bpy)_2(NH_3)_2]^{3+}$ with Cl_2, illustrating biphasic behavior. Data were extracted from the experiment for Figure 4. Note that the global fitting method used to analyze the kinetic data effectively achieves signal averaging over a 200-nm range, and hence the noise evident at 378.8 nm is much greater than that in the global fit.

to the fast process of the Ru(II) to Ru(III) oxidation, slower components are also evident. In this UV region both the reaction intermediates and the final product show strong absorbance. The Ru(III) intermediate produced within the first 250 ms duration was identified by comparing its characteristic UV spectrum with an authentic sample. These data clearly indicate that chemical oxidation of the *cis*-$[Ru(bpy)_2(NH_3)_2]^{2+}$ to the nitrosyl complex, *cis*-$[Ru(bpy)_2(NH_3)NO]^{3+}$, proceeds through the *cis*-$[Ru(bpy)_2(NH_3)_2]^{3+}$ intermediate. In order to understand the overall process thoroughly we have conducted an independent investigation of the reaction between *cis*-$[Ru(bpy)_2(NH_3)_2]^{3+}$ and Cl_2 in the UV region.

Reaction of *cis*-$[Ru(bpy)_2(NH_3)_2]^{3+}$ with Cl_2. The *cis*-$[Ru(bpy)_2(NH_3)_2]^{3+}$ solution used for the kinetic study was prepared *in situ* by oxidizing the *cis*-$[Ru(bpy)_2(NH_3)_2]^{2+}$ with MnO_2. No change on the kinetics has been observed upon conducting the oxidation with PbO_2. Thus, the effect of Mn^{2+} on the kinetics has been assumed to be minimal. Kinetic measurements were performed by following the absorbance change in the UV region (320−440 nm). Figure 4 shows a series of rapid-scan spectra recorded over a 15 s time period for a typical expermient, while Figure 5 shows the absorbance at 378.8 nm as a function of time for the same experiment. Oxidation of the coordinated ammonia by chlorine involves increasing absorbance in the

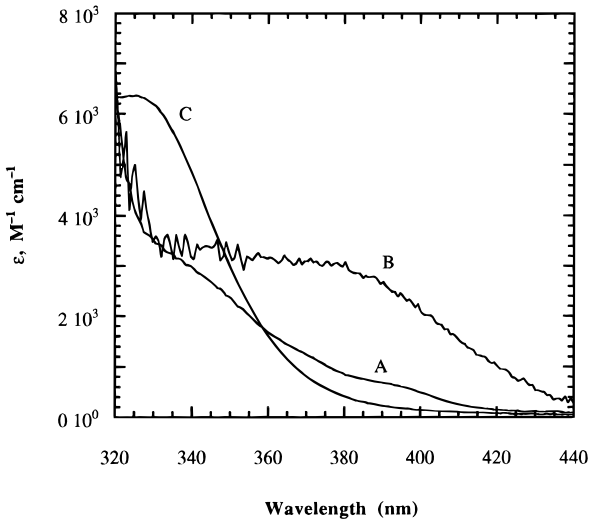

Figure 6. Spectral profile obtained from global fitting of the kinetics for the reaction between *cis*-$[Ru(bpy)_2(NH_3)_2]^{3+}$ and Cl_2; (a) spectrum of the Ru(III) reactant; (b) spectrum of the intermediate; and (c) spectrum of the final product. Conditions are the same as for Figure 4.

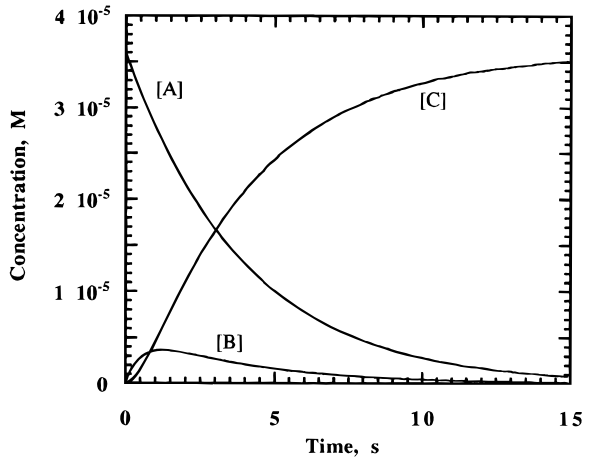

Figure 7. Kinetics fit for the consecutive reaction between *cis*-$[Ru(bpy)_2(NH_3)_2]^{3+}$ and Cl_2. Experimental conditions are as given in Figure 4.

320−350-nm region, and an initial fast increase is followed by a slow decrease in the 350−440-nm region. The reaction exhibits the features of two consecutive first-order processes and displays biphasic kinetics. A fairly significant difference in the two consecutive processes is apparent from the maintenance of isosbestic points at 322 and 352 nm at the later stage of the reaction. These qualitative spectral features are consistent with those obtained for the slower phases of the reaction when the starting material is Ru(II) rather than Ru(III). Quantitative treatment of the rapid-scan data was performed by use of the Specfit program[29] to compute global fits. These fits were based on a consecutive first-order kinetic scheme A → B → C under the constraint that the A → B step be the slow process, for reasons given below. Spectral profiles derived from these fits showing the starting species, the intermediate, and the final product are shown in Figure 6 for a typical example. Temporal profiles of the three species for this example are shown in Figure 7. The two rate constants deriving from each of the fits (k_{slow} and k_{fast}) are given in Table 3. Under conditions of low acidity with no added chloride the initial rapid phase (k_{fast}) was of too low amplitude to be detected, and the reaction was fit as single exponential function (k_{slow}).

Rate Law for the k_{slow} Process. A plot of k_{slow} vs $[Cl_2]_{tot}$ at constant $[H^+]$ and $[Cl^-]$ is linear with an intercept very close

Table 3. Dependence of k_{slow} and k_{fast} on $[H^+]$, $[Cl^-]$, and $[Cl_2]_{tot}$[a]

$[H^+]$, M	$[Cl_2]_{tot}$, mM	$[Cl^-]$, M	k_{slow}, s^{-1}	$k_{slow,calc}$, s^{-1}	k_{fast}, s^{-1}	$k_{fast,calc}$, s^{-1}
0.292	8.94[b]	0.208	0.22	0.20	2.0	1.89
0.152	7.97[b]	0.208	0.37	0.33	2.5	2.54
0.092	8.14[b]	0.208	0.57	0.55	3.1	3.29
0.043	8.31[b]	0.208	0.91	1.17	4.4	4.18
0.092	8.19[b]	0.208	0.56	0.56	3.2	3.31
0.095	5.16[b]	0.208	0.36	0.34	2.0	2.06
0.097	3.07[b]	0.208	0.26	0.20	1.0	1.21
0.091	9.94[b]	0.158	0.67	0.68	4.0	3.97
0.091	9.71[b]	0.108	0.64	0.64	4.8	3.77
0.092	10.73[b]	0.058	0.63	0.67	4.6	3.83
0.017[d]	3.72[c]	0.0035[e]	0.50	0.49	*f*	
0.036[d]	1.80[c]	0.0017[e]	0.15	0.13	*f*	
0.018[d]	5.20[c]	0.0048[e]	0.91	0.68	*f*	
0.018[d]	7.20[c]	0.0065[e]	1.29	1.01	*f*	
0.017[d]	20.4[c]	0.0162[e]	3.56	3.55	*f*	
0.014[d]	8.37[c]	0.0076[e]	1.41	1.44	*f*	
0.007[d]	9.80[c]	0.0092[e]	2.35	3.10	*f*	

[a] Conditions: $[Ru(III)]_0 = 0.06-0.08$ mM; $\mu = 0.5$ M ($LiClO_4$); 25 °C. [b] $[Cl_2]_{tot}$ calculated as $[HOCl] + [Cl_2]$, each being determined spectrophotometrically. [c] $[Cl_2]_{tot}$ calculated from the initial $[OCl^-]$. [d] Calculated from $[H^+] = [Cl_2]K_{Cl}/([HOCl][Cl^-])$, with $[Cl_2] = [Cl_2]_{tot} - [HOCl]$; these H^+ concentrations are in good agreement with those estimated from measured pH as 10^{-pH}. [e] Calculated by $[Cl^-] = [HOCl]$, the concentration of HOCl being determined from the absorbance at 254 nm. [f] Monophasic kinetics observed; k_{obs} assigned to k_{slow}.

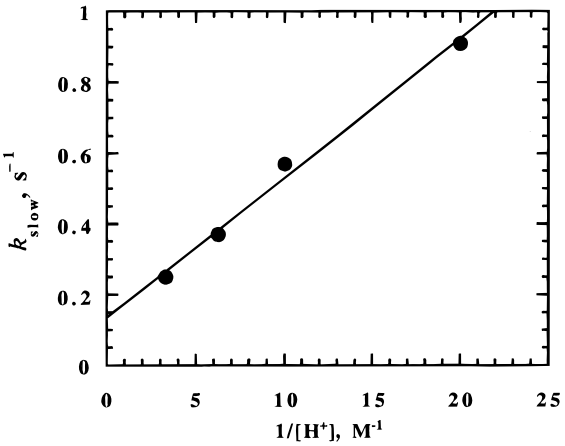

Figure 8. Plot showing the dependence of the k_{slow} process on $[H^+]$. The chloride concentration was kept constant (0.2 M) in these experiments. Other experimental conditions are as stated in Table 3 with $[Cl_2]_{tot} \sim 8$ mM.

to zero. However, the pH dependency of the rate is more complicated. In the pH range of 0.5−2.8 at constant $[Cl_2]_{tot}$ and $[Cl^-]$, the values of k_{slow} increase with a decrease in $[H^+]$. A plot of k_{slow} vs $1/[H^+]$ is linear (Figure 8) but provides a significant intercept, suggesting competitive pathways associated with this process. One likely possibility arises due to the hydrolysis of Cl_2 in aqueous media as in reaction 6. Depending upon the pH of the solution and chloride concentration either Cl_2 or HOCl could be the dominant species. Two experiments were designed in order to investigate the effect of the above equilibrium on the kinetics. The first experiment comprised a series of reactions conducted at high acid and chloride concentrations, whereas in the second set of experiments reactions were performed in the pH range of 1.7−2.8 with no added chloride. The dominant species in the former is Cl_2 while HOCl is the dominant species in the latter. The final reaction product in both cases has been confirmed to be the nitrosyl complex from its characteristic UV−absorption spectrum. At pH >3 a significant portion of the nitrosyl complex is converted to the nitrite form, which complicates the kinetics further. As a result we have analyzed the data corresponding only to the pH range of 0.5−2.8.

The kinetic studies conducted under the above conditions clearly indicate that both Cl_2 and HOCl react competitively with the deprotonated Ru(III) species, *cis*-$[Ru^{III}(bpy)_2(NH_3)(NH_2)]^{2+}$. The overall rate law for the k_{slow} process has the form

$$-\frac{d[Ru(III)]_{tot}}{dt} = \{k_2[Cl_2] + k_3[HOCl]\}\frac{[Ru(III)]_{tot}}{[H^+]} \quad (8)$$

Assuming,

$$[Cl_2]_{tot} = [Cl_2] + [HOCl] \quad (9)$$

and rewriting eq 6 in terms of K_{Cl}, rearranging and substituting into eq 9 provides eq 10:

$$[Cl_2] = \frac{[Cl_2]_{tot}[H^+][Cl^-]}{[H^+][Cl^-] + K_{Cl}} \quad (10)$$

This leads to

$$-\frac{d[Ru(III)]_{tot}}{dt} = \left\{\frac{k_2[H^+][Cl^-] + k_3K_{Cl}}{[H^+][Cl^-] + K_{Cl}}\right\}\frac{[Cl_2]_{tot}[Ru(III)]_{tot}}{[H^+]} \quad (11)$$

and hence,

$$k_{slow} = \left\{\frac{k_2[H^+][Cl^-] + k_3K_{Cl}}{K_{Cl} + [H^+][Cl^-]}\right\}\frac{[Cl_2]_{tot}}{[H^+]} \quad (12)$$

As shown in Table 3, a two-parameter nonlinear least-squares fit agrees very well with the observed data (using $K_{Cl} = 1.04 \times 10^{-3}$ M^2)[37] and provides values for k_2 and k_3 as 6.5 ± 0.3 and 2.0 ± 0.2 s^{-1}, respectively.

If it is assumed that the inverse acid dependence indicates reaction through a deprotonated form of Ru(III) existing as a minor component according to

$$cis\text{-}[Ru^{III}(bpy)_2(NH_3)_2]^{3+} \rightleftharpoons cis\text{-}[Ru^{III}(bpy)_2(NH_3)(NH_2)]^{2+} + H^+ \qquad K_{Ru} \quad (13)$$

then

$$[Ru^{III}-NH_2] = \frac{K_{Ru}[Ru(III)]_{tot}}{[H^+]} \quad (14)$$

Moreover, if it is assumed that Cl_2 and HOCl react independently with $[Ru^{III}-NH_2]$ with rate constants k_2' and k_3', then substituting eqs 9, 10, and 14 into eq 8 provides the overall rate law, eq 15.

$$-\frac{d[Ru(III)]_{tot}}{dt} = \left\{\frac{k_2'[H^+][Cl^-] + k_3'K_{Cl}}{[H^+][Cl^-] + K_{Cl}}\right\}\frac{[Cl_2]_{tot}K_{Ru}[Ru(III)]_{tot}}{[H^+]} \quad (15)$$

Comparison of eqs 15 and 11 makes the following identities: $k_2 = k_2'K_{Ru}$ and $k_3 = k_3'K_{Ru}$.

An estimate of K_{Ru} (eq 13) was obtained by following the change in $E_{1/2}$ of the cyclic voltammogram of a 1 mM solution of *cis*-$[Ru(bpy)_2(NH_3)_2]^{2+}$ ($\mu = 0.1$ M ($LiClO_4$)) with pH. In the pH range of 1−5.5 the reversible wave at $E_{1/2} = 0.86$ V

shows no significant shift, and indicates that the pK_{Ru} value for the reaction of eq 8 should be greater than 5.5. Based on previous studies on similar systems, (tpy)(bpy)Os(NH_3) (pK_a > 6.5)[16] and $[(bpy)_2(NH_3)Ru]_2O^{4+}$ (pK_a = 6.5),[21] a value of ca. 6.5 can be estimated for *cis*-$[Ru(bpy)_2(NH_3)_2]^{2+}$.

With the above estimate for the K_{Ru} value the rate constant corresponding to the Cl_2 pathway, k_2', is 2.1×10^7 M^{-1} s^{-1} and the k_3' value corresponding to the HOCl pathway is calculated as 6×10^6 M^{-1} s^{-1}. The data clearly indicate that the process involving Cl_2 is about four times faster than the rate corresponding to the HOCl reaction.

Rate Law for the k_{fast} Process. The values for k_{fast} correlate directly with $[Cl_2]$ and inversely with $[H^+]$, which implies that the intermediate participates in a preequilibrium to generate a deprotonated species that reacts with Cl_2. On the other hand, for a series of experiments at constant $[Cl_2]$ and $[H^+]$ there is no dependence on $[Cl^-]$, which indicates that the reaction of HOCl is negligible. The rate law for the k_{fast} process thus has the form

$$k_{fast} = \frac{k_4 K_{int}[Cl_2]_{tot}[H^+][Cl^-]}{\{K_{int} + [H^+]\}\{[H^+][Cl^-] + K_{Cl}\}} \qquad (16)$$

where K_{int} corresponds to the deprotonation pre-equilibrium constant and k_4 corresponds to the rate constant for the reaction of the deprotonated intermediate with Cl_2. As shown in Table 3, the data were rigorously fitted with a nonlinear least-square program, and the values of k_4 and K_{int} correspond to $(7.8 \pm 1.5) \times 10^2$ M^{-1} s^{-1} and 0.11 ± 0.04 M, respectively. The relatively large uncertainties in these parameters arise from the low resolution of the data: in all of the experiments the k_{fast} process is associated with small absorbance changes, and in several of the experiments it could not even be detected. A two-term rate law that adds a term corresponding to reaction of the deprotonated intermediate with HOCl gives only a modestly improved fit, and the value of the added rate constant is only marginally greater than its uncertainty. The fit with eq 16 indicates that the intermediate is fairly acidic with a pK_a value close to 1; with such a low pK_a this species could not be *cis*-$[Ru(bpy)_2(NH_3)_2]^{3+}$, and hence the k_{fast} step occurs second in the A → B → C sequence. Despite the large value of K_{int}, spectra of the intermediate do not show large changes as a function of pH. The identity of the intermediate is discussed below.

Discussion

Product Characterization. The nitrosyl product for the oxidation of coordinated ammonia in *cis*-$[Ru(bpy)_2(NH_3)_2]^{2+}$ by Cl_2 was characterized using various spectroscopic techniques. Infrared spectroscopic studies of the product provide a strong ν(NO) stretching band at 1944 cm^{-1}. The result is consistent with previous assignments for $[Ru^{II}(bpy)_2Cl(NO)]^+$ complexes[38] where the ν(NO) stretching frequency of the cis geometry (1934 cm^{-1}) occurs 20 cm^{-1} higher than for the trans isomer. In addition, a cis arrangement for the nitrosyl ligand is also inferred from the ^{1}H NMR studies. As discussed earlier, the nonequivalent environment that arises when the two bpy ligands are placed in a cis arrangement is evident from the ^{1}H NMR data since out of a total of 16 proton resonances, 12 distinct bands were observed. Moreover, UV−vis absorption and CV studies (Table 1) provide results consistent with previous studies on the *cis*-$[Ru(bpy)_2(NH_3)NO]^{3+}$ system.[19,26] In addition, a FAB mass spectrometry study conducted on *cis*-$[Ru(bpy)_2(NH_3)NO]^{3+}$ shows a distinctive set of ions with *m*/*e* corresponding to the parent and fragments of the parent derived by loss of NH_3, NO, and bpy ligands. The parent ion is observed in the reduced form as $[Ru(bpy)_2(NH_3)(NO)ClO_4]^+$ at 560 *m*/*e*, whereas fragments corresponding to the ions $[Ru(bpy)_2(NO)]^+$, $[Ru(bpy)_2]^+$, and $[Ru(bpy)(NOH)]^+$ were observed at 444, 413, and 288 *m*/*e*, respectively. These results are further supported by the satisfactory microchemical analysis obtained on the compound.

Kinetics. As mentioned in the introduction, a variety of mechanisms have been proposed for the oxidation of coordinated ammonia. These generally include one-electron oxidation from the M(II) to M(III) stage, followed by a variety of processes including further one-electron oxidation, deprotonation, disproportionation, electrophilic attack, and complex electrode reactions. Some degree of simplification has been achieved in reactions of coordinated organic amines, where oxidative dehydrogenation is the norm. Thus, net conversion of chelated amines to imines has been reported as far back as 1966.[39] Subsequent studies indicate that the oxidative dehydrogenation of amines is assisted by coordinated metal ions.[40] Macrocyclic amine complexes of Ni^{2+}, Cu^{2+}, and Fe^{2+} have been reported to undergo oxidative dehydrogenation where the net reaction involves prior oxidation of the metal center followed by oxidation of the ligand and reduction of the metal ion.[41,42] Primary amines bound to the $[Ru^{II}(bpy)_2]$ moiety also undergo oxidative dehydrogenation.[43] In cases where the amine ligands lack α-CH groups, oxidation can lead to stable amido complexes.[44] By the use of rapid-scan stopped-flow methods, we now show that the oxidation of coordinated ammonia by aqueous chlorine proceeds through a series of stages with well-defined rate laws and mechanisms.

The first observable stage in the chemical oxidation of the *cis*-$[Ru(bpy)_2(NH_3)_2]^{2+}$ by aqueous Cl_2 is consistent with previous electrochemical investigations in that it involves the metal-centered oxidation (as shown in eq 3) of Ru(II) to Ru(III). Moreover, the rate law indicates a rate-limiting step involving the direct interaction of molecular Cl_2 with *cis*-$[Ru(bpy)_2(NH_3)_2]^{2+}$. Inasmuch as the Ru(II) reactant is substitution inert, the most-likely mechanism for this first stage is a pair of one-electron-transfer reactions, as given below:

$$cis\text{-}[Ru(bpy)_2(NH_3)_2]^{2+} + Cl_2 \underset{k_{-1}}{\overset{k_1}{\rightleftharpoons}} cis\text{-}[Ru(bpy)_2(NH_3)_2]^{3+} + Cl_2^- \qquad K_1 \quad (17)$$

$$cis\text{-}[Ru(bpy)_2(NH_3)_2]^{2+} + Cl_2^- \rightarrow cis\text{-}[Ru(bpy)_2(NH_3)_2]^{3+} + 2Cl^- \qquad k_2 \quad (18)$$

This mechanism leads to the observed rate law, eq 5′, when the first step is rate limiting. In order for this to be the case, the steady-state approximation requires that $k_{-1}[Ru(III)] \ll k_2[Ru(II)]$. We can estimate that the value of k_2 exceeds 1.6×10^9 M^{-1} s^{-1}, which is the rate constant for the corresponding reaction of Cl_2^- with $[Ru(bpy)_3]^{2+}$, a significantly weaker

(38) Nagao, N.; Nishimura, H.; Funato, H.; Ichikawa, Y.; Howell, F. S.; Mukaida, M.; Kakihana, H. *Inorg. Chem.* **1989**, *28*, 3955−3959.

(39) Curtis, N. F. *J. Chem. Soc., Chem. Commun.* **1966**, 881−883.

(40) Brown, G. M.; Weaver, T. R.; Keene, F. R.; Meyer, T. J. *Inorg. Chem.* **1976**, *15*, 190−196.

(41) Goedken, V. L.; Busch, D. H. *J. Am. Chem. Soc.* **1972**, *94*, 7355−7363.

(42) Dabrowiak, J. C.; Lovecchio, F. V.; Goedken, V. L.; Busch, D. H. *J. Am. Chem. Soc.* **1972**, *94*, 5502−5504.

(43) Keene, F. R.; Salmon, D. J.; Meyer, T. J. *J. Am. Chem. Soc.* **1976**, *98*, 1884−1889.

(44) Chiu, W.-H.; Peng, S.-M.; Che, C.-M. *Inorg. Chem.* **1996**, *35*, 3369−3374.

reducing agent.[45] An estimate of k_{-1} can be derived from the measured value of k_1, the principle of detailed balancing, and the value of K_1, which can be calculated from values of $E°$ for the corresponding Ru(III)/Ru(II) and Cl_2/Cl_2^- redox couples. There is considerable uncertainty in $E°$ for the Cl_2/Cl_2^- couple, with reported values ranging from 0.70 to 0.43 V.[46,47] (Note: Our prior estimate[46] of this potential overlooked the conflicting report of Thornton et al.;[47] the origin of the disagreement is unclear.) So long as the true potential lies within these extremes, reaction 17 is an uphill process. Use of the lower $E°$ value leads to a value for k_{-1} that is too fast (2×10^{10} M^{-1} s^{-1}), but the higher $E°$ value gives a value of k_{-1} that is compatible with the demands of the steady-state approximation and the first-order kinetic dependence on [Ru(II)]. We infer that the Cl_2/Cl_2^- potential is greater than 0.43 V and thus that the mechanism in reactions 17 and 18 is plausible.

It is reasonable to describe reaction 17 as an outer-sphere electron-transfer reaction, although some degree of orbital overlap between Cl_2 and the aromatic ligands may occur. By way of comparison, the only other reported reaction of Cl_2 with substitution-inert transition-metal complex having no vacant coordination sites is that with $[Fe(phen)_3]^{2+}$.[48,49] A 460-fold lower rate constant is reported for the reaction of Cl_2 with $[Fe(phen)_3]^{2+}$ (2.4 M^{-1} s^{-1}), which is qualitatively in agreement with expectations based on the greater thermodynamic barrier for this reductant. Detailed calculations in terms of Marcus theory would be of interest, but they should be deferred until a reliable potential for the Cl_2/Cl_2^- couple becomes available. Irrespective of the exact potential for the Cl_2/Cl_2^- couple, the values of k_1 and $E°$ for the two metal complexes allow us to calculate that the oxidation of Cl_2^- to Cl_2 has a rate constant (k_{-1}) that is 5-fold greater for the reaction with $[Fe(phen)_3]^{3+}$ than for *cis*-$[Ru(bpy)_2(NH_3)_2]^{3+}$.

A mechanism for the subsequent phases of the reaction of $[Ru(bpy)_2(NH_3)_2]^{3+}$ with aqueous chlorine that is consistent with the observed rate laws is presented in Scheme 1.

Scheme 1

$$Ru^{III}-NH_3 \underset{+H^+}{\overset{-H^+}{\rightleftharpoons}} Ru^{III}-NH_2 \qquad K_{Ru} \qquad (19)$$

$$Ru^{III}-NH_2 \xrightarrow{Cl_2} Ru_{int1} \qquad k_2 \qquad (20)$$

$$Ru^{III}-NH_2 \xrightarrow{HOCl} Ru_{int1} \qquad k_3 \qquad (21)$$

$$Ru_{int1} \underset{+H^+}{\overset{-H^+}{\rightleftharpoons}} Ru_{int2} \qquad K_{int} \qquad (22)$$

$$Ru_{int2} \xrightarrow{Cl_2} Ru^{II}-NO^+ \qquad k_4 \qquad (23)$$

Deducing an overall mechanism for the reaction past the Ru(II) to Ru(III) stage has been complicated as we were not able to identify all of the possible intermediates for this multielectron process. Other intermediates that have been proposed[16] in electrochemical studies of this multielectron oxidation process include $\{Ru^{IV}{=}NH\}$, $\{M^{II}NH_2O\}$, $\{M^{II}NHO\}$, and $\{M^{II}NO^{\bullet}\}$ species. Our attempt to observe some of these intermediates has not been successful in this study. For example the $\{M^{II}NH_2O\}$ intermediate, which would be expected to show an intense absorption band corresponding to the $d(Ru^{II}) \rightarrow \pi^*$-(bpy) transition in the visible region, has not been observed in the fast kinetic studies and may indicate that either this intermediate does not accumulate in any significant amount or the chemical oxidation by Cl_2 does not proceed through such an intermediate. In fact, Margerum et al. have found that various alkylamines (including ammonia) react with Cl_2 nearly at a diffusion-controlled rate to form chloroamines.[50] Reaction of free ammonia with HOCl is nearly three orders of magnitude slower than the corresponding reaction with Cl_2. Moreover the rate constant for the HOCl reaction increases as the basicity of the amines increases suggesting a nucleophilic attack by the amine on the Cl atom in HOCl as the rate-determining step (Cl^+ transfer mechanism). In view of these observations and the unique ability of aqueous chlorine to effect this oxidation, it is likely that the observed intermediates, Ru_{int1} and Ru_{int2}, in this reaction are chloroamine complexes. This assignment is supported by the low pK_a of Ru_{int1}, since chloramines are generally much weaker bases than their corresponding amines.[50] Further support comes from reports that aqueous chlorine reacts with Pt(IV) ammines to give dichloramido complexes.[13,14] On the other hand, oxidation of ammonia in Cr and Mn systems by Cl_2 has been found to provide the corresponding nitrido complexes.[7,8,51] Even though we have not been able to identify the nature of the intermediate, we are able to infer that the intermediate of this reaction is highly acidic with a pK_a value close to 1. The high acidity of the intermediate species might indicate that the nitrido system is an unlikely intermediate in the ruthenium reactions.

If the assignment of Ru_{int1} as a coordinated chloramine is correct, then the final stage in the mechanism (reaction 23) has the overall stoichiometry

$$cis\text{-}[Ru^{III}(bpy)_2(NH_3)(NHCl)]^{2+} + {}^3/_2Cl_2 + H_2O \rightarrow cis\text{-}[Ru^{II}(bpy)_2(NH_3)(NO)]^{3+} + 4Cl^- + 3H^+ \qquad (24)$$

This obviously requires a multistep mechanism, and the rate law requires reaction with Cl_2 as the first step. Further information is required to determine whether this occurs through an electron-transfer mechanism, in analogy with the reaction of Cl_2 with *cis*-$[Ru^{II}(bpy)_2(NH_3)_2]^{2+}$, or through a Cl^+ transfer mechanism. Among the subsequent steps, one likely possibility is hydrolysis, as is suggested by the known hydrolysis of chloramine:[52]

$$NH_2Cl + OH^- \rightarrow NH_2OH + Cl^- \qquad (25)$$

Irrespective of the mechanistic details, a potentially important fact emerges when this reaction is compared with the reaction of aqueous ammonia with acidic chlorine. This latter reaction generates chloramine and has the rate law

$$-d[NH_4^+]/dt = (k_{Cl}K_N[Cl_2] + k_{OCl}K_N[HOCl])[NH_4^+]/[H^+] \qquad (26)$$

where $k_{Cl}K_N = 1.9$ s^{-1} and $k_{OCl}K_N = 1.4 \times 10^{-3}$ s^{-1}.[50] In this expression, k_{Cl} is the second-order rate constant for direct reaction of Cl_2 with NH_3, k_{OCl} is the second-order rate constant

(45) Mulazzani, Q. G.; Venturi, M.; Bolletta, F.; Balzani, V. *Inorg. Chim. Acta* **1986**, *113*, L1−L2.
(46) Stanbury, D. M. *Adv. Inorg. Chem.* **1989**, *33*, 69−138.
(47) Thornton, A. T.; Laurence, G. S. *J. Chem. Soc., Dalton Trans.* **1973**, 1632−1636.
(48) Ige, J.; Ojo, J. F.; Olubuyide, O. *Can. J. Chem.* **1979**, *57*, 2065−2070.
(49) Shakhashiri, B. Z.; Gordon, G. *Inorg. Chem.* **1968**, *7*, 2454−2456.
(50) Margerum, D. W.; Gray, E. T.; Huffman, R. P. In *Organometals and Organometalloids*; Brinckman, F. E., Bellama, J. M., Eds.; American Chemical Society: Washington, DC, 1978; pp 278−291.
(51) Dehnicke, K.; Strähle, J. *Angew. Chem., Int. Ed. Engl.* **1992**, *31*, 955−978.
(52) Anbar, M.; Yagil, G. *J. Am. Chem. Soc.* **1962**, *84*, 1790−1796.

for direct reaction of HOCl with NH_3, and K_N is the acid dissociation constant for NH_4^+. Casting the rate law in this form makes it possible to draw direct comparisons with the reaction of *cis*-$[Ru(bpy)_2(NH_3)_2]^{3+}$ with aqueous chlorine as in eq 8, since they have the same algebraic form. The ratio $k_2/(k_{Cl}K_N)$ has a value of 3.4, while a value of 1.4×10^3 is obtained for $k_3/(k_{OCl}K_N)$. These ratios show that coordination of ammonia to Ru(III) activates it with respect to reaction with aqueous chlorine. The effect most likely derives from the greater acidity of $Ru^{III}-NH_3$ relative to NH_4^+, and it has its origins in the greater charge on Ru(III). These insights suggest that other highly charged metal ions could also activate ammonia in this reaction, as appears to be the case for Pt(IV).[13,14] This may be of significance in water-treatment systems, where ammonia is often present during the chlorination process.[53]

(53) White, G. C. *The Handbook of Chlorination;* 2nd ed.; Van Nostrand Reinhold Co.: New York, 1986; pp 160−177.

Conclusion. Oxidation of coordinated ammonia in *cis*-$[Ru(bpy)_2(NH_3)_2]^{2+}$ by acidic aqueous chlorine provides the nitrosyl complex, *cis*-$[Ru(bpy)_2(NH_3)(NO)]^{3+}$, as the final product. The first step in this process involves the metal centered oxidation of *cis*-$[Ru(bpy)_2(NH_3)_2]^{2+}$ to *cis*-$[Ru(bpy)_2(NH_3)_2]^{3+}$. Independent studies conducted on the *cis*-$[Ru(bpy)_2(NH_3)_2]^{3+}$ complex show that conversion to the nitrosyl follows an A → B → C type consecutive pathway with k_{slow} and k_{fast} components, respectively. In the pH range of 0.5−2.8, the k_{slow} process follows a competitive pathway where both Cl_2 and HOCl react with the deprotonated *cis*-$[Ru(bpy)_2(NH_3)NH_2]^{2+}$ complex. The k_{fast} process involves a fast preequilibrium, involving deprotonation of the intermediate, followed by a direct attack by Cl_2.

Acknowledgment. This research was supported by the National Science Foundation. D.M.S. is a Sloan Research Fellow.

JA9633629